Fine structure of Vavilov-Cherenkov radiation near the Cherenkov threshold

V.G. Kartavenko [a,b,1], G.N. Afanasiev [a,1] and W. Greiner [b]

[a] *Bogoliubov Laboratory of Theoretical Physics, Joint Institute for Nuclear Research, Dubna, Moscow District, 141980, Russia*

[b] *Institut für Theoretische Physik der J. W. Goethe Universität D-60054 Frankfurt am Main, Germany*

Abstract

We analyze the Vavilov-Cherenkov radiation (VCR) in a dispersive nontransparent dielectric air-like medium both below and above the Cherenkov threshold, in the framework of classical electrodynamics. It is shown that the transition to the subthreshold energies leads to the destruction of electromagnetic shock waves and to the sharp reduction of the frequency domain where VCR is emitted. The fine wake-like structure of the Vavilov-Cherenkov radiation survives and manifests the existence of the subthreshold radiation in the domain of anomalous dispersion. These domains can approximately be defined by the two phenomenological parameters of the medium, namely, the effective frequency of oscillators and the damping describing an interaction with the other degrees of freedom.

PACS: 41.60.Bq

Key words: Cherenkov radiation; Cherenkov threshold; Fine structure

[1] Corresponding author. Phone: +7 09621 63710; Fax: +7 09621 65084;
E-mail: kart@thsun1.jinr.ru

1 Introduction

Vavilov-Cherenkov radiation (VCR) is a well established phenomenon widely used in physics and technology [1,2]. Nevertheless, some of its fundamental aspects are still open. Recently, interest in the problem of surpassing the Cherenkov threshold has been renewed. A group of researchers from Comenius Univercity, Bratislava, CERN and JINR have carried out measurements of VCR induced by a high-energy beam of lead ions in air, helium and various crystals (NA49 experiment) [3]. The members of this group supposed [4], using the previously obtained experimental data on VCR induced by relativistic electrons in air [5], that the pre-Cherenkov electromagnetic shock wave could arise when the charge particle velocity v coincides with the phase velocity of light in the medium $c_n = c/n_0$ (n_0 is the refractive index of the medium, and c denotes light velocity in the vacuum). For a relativistic electron moving in a gas the radiation intensity was measured as a function of a gas pressure P, which is related in a simple way to the gas refractive index n_0. Changing continuously the refractive index of the medium one gets a tool to analyse VCR both below and above the Cherenkov threshold. A small but finite value of intensity indicates the existence of VCR below the threshold velocity $v < c_n$ [5]. In spite of the fact that these experiments are preliminary, it is useful to conduct a detailed theoretical analysis of VCR both below and above the Cherenkov threshold. It is the goal of this paper.

We investigate electromagnetic fields (EMF) radiated by a point charge uniformly moving in a dielectric dispersive medium. It is suggested that uniform motion of a particle is maintained by some external force whose origin is not of interest for us. In the case of frequency independent electric permittivity $\epsilon_0 = \sqrt{n_0}$, there is no electromagnetic field (EMF) before the Cherenkov cone accompanying the charge, an infinite EMF on the Cherenkov cone itself and finite values of EMF strengths behind it [6,7]. So information concerning the transition effects arising when charge velocity coincides with c_n is lost (except for the existence of the Cherenkov shock wave itself) [8].

In the classical electrodynamics [2,9] VCR is a collective phenomenon involving a large number of atoms of the medium whose electrons are excited by EMF of the passing particle. Therefore, we use the macroscopic complex dielectric function ϵ [9,10]

$$\epsilon(\omega, p) = 1 + \frac{\omega_L^2}{\omega_0^2 - \omega^2 + ip\omega}. \tag{1}$$

This is the standard parameterization describing many optical phenomena [11] and is well suited for air-like media investigated in [4]. Following [12,13], we extrapolate the parameterization (1) to all ω. This means that we disregard

the excitation of nuclear levels and the discrete structure of scatterers.

2 Electromagnetic fields

The charge and current densities of the treated problem, Fig. 1, are given by [2] $\rho(\vec{r},t) = e\delta(x)\delta(y)\delta(z-vt),\ j_z = v\rho$. The cylindrical components of EMF strengths can be written in the following form [14]

$$
\begin{aligned}
H_\phi &= \frac{2e}{\pi v c}\int\limits_0^\infty d\omega\omega|1-\beta^2\epsilon|^{1/2}\Big((\cos(\frac{\phi}{2}+\alpha)K_{1r} - \sin(\frac{\phi}{2}+\alpha)K_{1i}\Big),\\
E_z &= -\frac{2}{\pi v^2}\int\limits_0^\infty d\omega\omega\Big(\Big(\cos\alpha(\epsilon_r^{-1}-\beta^2) - \epsilon_i^{-1}\sin\alpha\Big)K_{0i}\\
&\quad + \Big(\sin\alpha(\epsilon_r^{-1}-\beta^2) + \epsilon_i^{-1}\cos\alpha\Big)K_{0r}\Big),\\
E_\rho &= \frac{2}{\pi v^2}\int\limits_0^\infty d\omega\omega|1-\beta^2\epsilon|^{1/2}\Big((\epsilon_r^{-1}\cos\alpha - \epsilon_i^{-1}\sin\alpha)(\cos\frac{\phi}{2}K_{1r} - \sin\frac{\phi}{2}K_{1i})\\
&\quad - (\epsilon_i^{-1}\cos\alpha + \epsilon_r^{-1}\sin\alpha)(\sin\frac{\phi}{2}K_{1r} + \cos\frac{\phi}{2}K_{1i})\Big). \qquad (2)
\end{aligned}
$$

$$
\begin{aligned}
&K_{mr} = ReK_m(\frac{\rho\omega}{v}\sqrt{1-\beta^2\epsilon}), \quad K_{mi} = ImK_m(\frac{\rho\omega}{v}\sqrt{1-\beta^2\epsilon}), \quad \mathrm{m} = 0,1\\
&\alpha \equiv \omega(t-z/v), \quad \epsilon_r \equiv Re\epsilon, \quad \epsilon_i \equiv Im\epsilon,\\
&\phi \equiv \arg\left(1-\beta^2\epsilon\right), \quad Re\sqrt{1-\beta^2\epsilon} > 0.
\end{aligned}
$$

We present here only a minimal set of mathematical relations to evaluate EMF. For mathematical details (derivation of equations, analysis of possible divergences, semiclassical WKB estimates, gauge and polarization selections, Kronig-Kramers dispersion relations etc.) we refer to [14,15].

The time dependence of EMF strengths at the surface of the cylinder C_ρ ($\rho = 10\,[c/\omega_0],\ z = 0$), induced by a fast particle moving along the "z" axis is exhibited in Figs. 2 and 3. To describe the passing of a light barrier by a charge particle in the experiments [4], we select the following parameters. The pressure is related to the gas density N_g by the well-known thermodynamic

[2] We follow the original papers of Tamm-Frank [7] and Fermi [10] to treat VCR. The important peculiarities of the VCR near the Cherenkov threshold due to a finite thickness of the radiator [16–19] and possible effects due to accelerated and decelerated motion [8] will be considered separately.

relation: $PV = kN_gT$, where V is the gas volume, T is its temperature and k is the Boltzmann constant. In the definition of ϵ (1) ω_L is the plasma frequency $\omega_L^2 = 4\pi N_e e^2/m$, $N_e = N_g Z$ is the number of electrons per unit of volume, m is the electron mass, ω_0 is some resonance frequency and Z is the atomic number of the gas particles. The particle velocity is $\beta \sim 0.999$. The Cherenkov threshold can be associated with the critical velocity $\beta_c \equiv \sqrt{1/\epsilon(0,0)}$ [14]. Changing β_c from 0.99 to 0.9999, describes a transition from the superlight regime to the sublight one, and corresponds to an approximately 100 time decrease in the gas pressure.

In Figs. 2 and 3 one can see formation of the well-defined front of electromagnetic shock waves for $\beta > \beta_c$ and suppression of a pre-front wave structure which existed for $\beta < \beta_c$.

A fine structure of EMF strengths presented in Figs. 2 and 3 indicates that the response of a dispersive medium to a penetrating charge particle manifests itself in an axially symmetrical wake-like [20] space-time distribution. These are well-known properties, in the case of $\beta > \beta_c$, of any homogeneous isotropic electron plasma with a dielectric function $\epsilon(\omega, 0)$ [21–23]. We will use the terminology of "wake", although the Cherenkov cone does not exist for subthreshold velocities $\beta < \beta_c$.

3 The radiated EMF energy flux

The energy flux per unit length radiated through the surface of a cylinder C_ρ (Fig. 1) coaxial with the z axis for the total time of motion is given by Poynting's vector $S_\rho = -(c/4\pi)E_z H_\phi$

$$W_\rho = \int_{-\infty}^{+\infty} \sigma_\rho dt = \frac{1}{v} \int_{-\infty}^{+\infty} \sigma_\rho dz, \quad \sigma_\rho = 2\pi\rho S_\rho. \tag{3}$$

Time dependence of EMF flux densities $\vec{\sigma}(t)$ is presented in Fig. 4. One can see very different time distributions for subthreshold and normal regimes. The EMF flux is localized more strongly than the EMF strengths. It is a result of complicated interference of electric and magnetic strengths entering via Eq (3) in the definition of Poynting's vector.

Using E_z and H_ϕ given by (2) for the whole time of charge motion one gets $W_\rho = \int_0^\infty f_\rho(\omega) d\omega$, where the ρ component of a spectral density is given by [14]

$$f_\rho(\omega) = -\frac{2e^2\rho}{\pi v^3}\omega^2|1-\beta^2\epsilon|^{1/2}\times$$
$$\times\Big((K_{0r}K_{1r}+K_{0i}K_{1i})\Big((\epsilon_r^{-1}-\beta^2)\sin\frac{\phi}{2}-\epsilon_i^{-1}\cos\frac{\phi}{2}\Big)$$
$$-(K_{0i}K_{1r}-K_{0r}K_{1i})\Big((\epsilon_r^{-1}-\beta^2)\cos\frac{\phi}{2}+\epsilon_i^{-1}\sin\frac{\phi}{2}\Big)\Big). \quad (4)$$

At a large distance in the limit $p \to 0$ this expression turns into the well-known relations [7]

$$\lim_{p\to 0} f_\rho(\omega) = 0, \quad for\ \beta^2\epsilon < 1,$$
$$\lim_{p\to 0} f_\rho(\omega) = \frac{e^2\omega}{c^2}(1-\frac{1}{\epsilon\beta^2}), \quad for\ \beta^2\epsilon > 1,$$
$$\lim_{p\to 0} W_\rho = \frac{e^2}{c^2}\int\limits_{\beta^2\epsilon>1}\omega d\omega(1-\frac{1}{\epsilon\beta^2}). \quad (5)$$

The validity of Eq. (5) has been confirmed in [10,24].

In Fig. 5, we present the radiated energy losses per unit length W_ρ on a cylinder C_ρ as a function of a particle velocity for a few parameters of β_c. One can see that for the fixed permittivity of the medium there exist radiated energy losses for the subthreshold velocities. The increasing damping reduces domains of a particle velocity with an essential VCR.

The spectral distributions $f_\rho(\omega)$ of the radiated energy losses are shown in Fig. 6. The numbers of particular curves mean β. It is seen that for $\beta > \beta_c$ all ω from the interval $0 < \omega < \omega_0$ contribute to the energy losses. For $\beta < \beta_c$ the interval of permissible ω diminishes. The spectral density $f_\rho(\omega)$ of the radiated energy losses defines the corresponding photon number spectral density $n_\rho(\omega) \equiv f_\rho(\omega)/\hbar\omega$ and the total number of photons emitted per unit length $N_\rho = \int_0^\infty d\omega n_\rho(\omega)$.

In Fig. 6, one can see that the damping parameter reduces the high frequency part $\omega \sim \omega_0$ of the domains where VCR is emitted. Fig. 5 shows that the damping strongly reduces the radiated energy losses especially for the low velocities. Spectral domains of VCR can approximately be fixed by the condition $Re(\epsilon) > \beta^{-2}$. These domains are defined by the two phenomenological parameters of the medium, namely, the effective frequency ω_0 of oscillators and the damping p describing interactions with the other degrees of freedom. The evaluated photon number spectral density $n_\rho(\omega)$ and the total number of photons emitted per unit length N_ρ look very much like the corresponded spectral distributions $f_\rho(\omega)$ and the radiated energy losses W_ρ, respectively. To not overload the composition, we don't present the figures for $n_\rho(\omega)$ and N_ρ.

It follows from Fig. 4 that rapid oscillations of the radiation intensity as a function of time should be observed in a particular detector. To detect S_ρ, one should have a detector imbedded into a thin collimator and directed towards the charge motion axis. The collimator should be impenetrable for the γ quanta with directions different from the radial one. The semiclassical WKB estimation [14] for a period $T \approx 2\pi/(\epsilon_0\omega_0)$ or the counting of the peaks in Fig. 4 gives $T \sim 10^{-15}$ *sec*. It seems that these oscillations shown in Fig. 4 for air-like media could be very difficult to resolve experimentally.

4 Conclusion

We have evaluated electromagnetic potentials, strengths and Poynting's vector describing space-time distribution of EMF induced in the air-like medium by a fast charge particle both below and above the Cherenkov threshold.

In the case of $\beta > \beta_c$ the response of a dispersive medium to a penetrating charge particle manifests itself in the formation of a sharp front and rapid wake-like oscillations behind the moving charge indicating the appearance of electromagnetic shock waves. A fine structure of EMF for $\beta < \beta_c$ manifests in the existence of EMF radiation under the Cherenkov threshold in the domain of anomalous dispersion.

We have calculated the spectral distributions, the number of the emitted photons and the radiated EMF energy flux. It is shown that the transition to the subthreshold regime ($\beta > \beta_c \rightarrow \beta < \beta_c$) and the damping ($p \neq 0$) lead to the sharp reduction of the anomalous frequency range where VCR is emitted.

We acknowledge valuable discussions with Prof. V.P. Zrelov and Prof. J. Ruzičkа. Authors are thankful to Prof. R. Gupta for his constructive criticisms of the manuscript.

References

[1] I.M. Frank, *Vavilov-Cherenkov Radiation*, (Moscow, Nauka, 1988).

[2] W. Greiner, *Classical Electrodynamics* (Springer, N.Y., 1998).

[3] CERN Courier, **39** No.9, 7 (1998).

[4] A.A. Tyapkin , J. Ruzicka, and V.P. Zrelov, JINR Rapid Comm., **1[87]-98**, 10 (1998).

[5] J.Ruzicka, "Theoretical and experimental investigation of the Vavilov-Cherenkov effect", Dsc Dissertation, JINR Dubna, 1993.

[6] D. Heaviside, *Electromagnetic Theory*, vol. 3, (London, The Electrician, 1912).

[7] I.M. Frank and I.E. Tamm, Dokl. Acad. Nauk SSSR, **14**, 107 (1937).

[8] G.N. Afanasiev, S.M. Eliseev, and Y.P. Stepanovsky, Proc. R. Soc. Lond., **A 454**, 1049 (1998).

[9] A.I. Akhiezer and N.F. Shulga N.F., *High Energy Electrodynamics in Medium*, (Moscow, Nauka. 1993).

[10] E. Fermi, Phys. Rev., **57**, 485 (1940).

[11] M. Born and E. Wolf, *Principles of Optics*, (Oxford, Pergamon, 1975).

[12] L. Brillouin, *Wave Propagation and Group Velocity*, (N.Y. and London, Academic Press, 1960).

[13] A. Lagendijk and B.A. Van Tiggelen, Physics Reports, **270**, 143 (1996).

[14] G.N. Afanasiev, and V.G. Kartavenko, J. Phys. D: Appl. Phys. **31**, 2760 (1998).

[15] G.N. Afanasiev, V.G. Kartavenko, and E.M. Magar, Preprint JINR **E2-98-98** (1998), (Physica B, in press)

[16] I.E. Tamm, J. Phys. USSR **1**, 439 (1939).

[17] V.E. Pafomov, Soviet Physics JETP **6**, 1079 (1958).

[18] D.K. Aitken, R.E. Jennings, A.S.L. Parsons, and R.N.F. Walker, Proc. Phys. Soc. **82**, 710 (1963).

[19] A.P. Kobzev, and I.M. Frank, Sov. J. Nucl. Phys. **34**, 125 (1981).

[20] V.N. Neelavathie, R.H. Ritchie, and W. Brandt, Ann. Phys. (N.Y.) **6**, 1 (1959).

[21] D. Bohm D. and D. Pines, Phys. Rev., **82** 625 (1951); ibid. **85**, 338 (1952).

[22] H. Rothard H. *et al.*, J. Physique Coll., **48 C** 211 (1988).

[23] W. Schäfer, H. Stöcker, and W. Greiner, Z. Phys. A, **288**, 349 (1978); Z. Phys. B, **36**, 319 (1980).

[24] V.L. Ginzburg, 1996, Usp. Fiz. Nauk, No**10**, 1033 (1996).

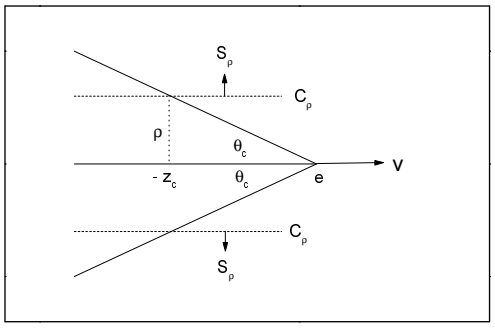

Fig. 1. The problem under consideration: an electron moves in a medium in positive z-direction with constant velocity v (ρ and z are cylindrical coordinates in the projectile rest frame). The Cherenkov cone is presented schematically for a medium of a constant dielectric coeficient. $\theta_c = \arcsin(c_n/v)$ is the Cherenkov angle. On the surface of the cylinder C_ρ EMF is zero for $z > -z_c$. The component S_ρ of Poynting's vector describes EMF energy flux through the surface of the cylinder, which confined to the surface of the cone. EMF inside the cone does not contribute to the radiation.

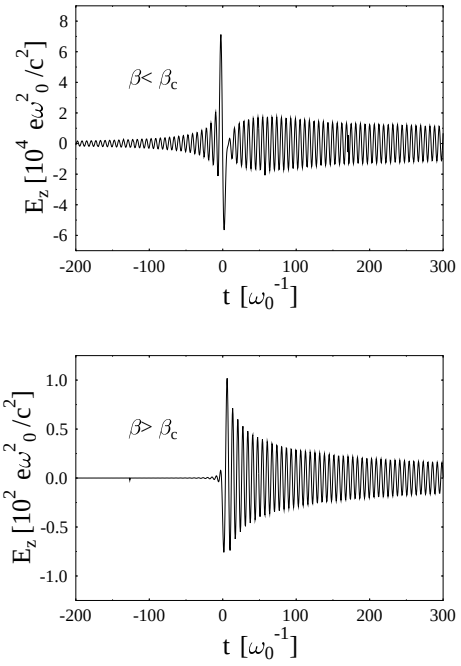

Fig. 2. Time dependence of the electric field strength on the surface of the cylinder C_ρ both below and above Cherenkov threshold.

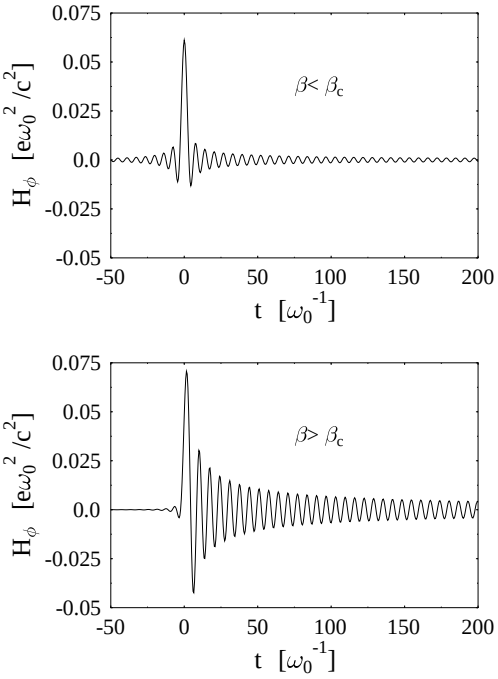

Fig. 3. Time dependence of the magnetic field strength on the surface of the cylinder C_ρ.

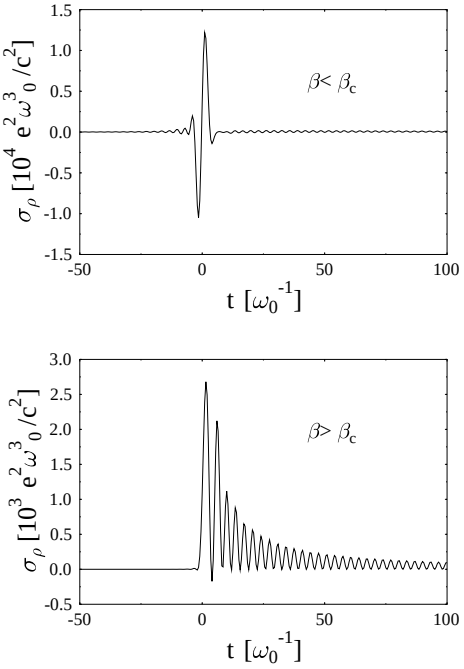

Fig. 4. Time dependence of the radiated EMF energy flux per unit length of the surface of the cylinder C_ρ both below and above Cherenkov threshold.

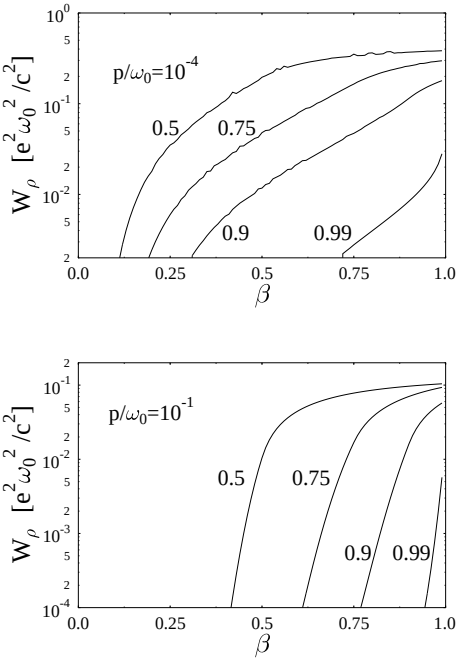

Fig. 5. The radiated energy losses per unit length as a function of a electron velocity for two damping parameters. The numbers on a particular line means β_c (a static refractive index of a media $n_0 = 1/\beta_c$).

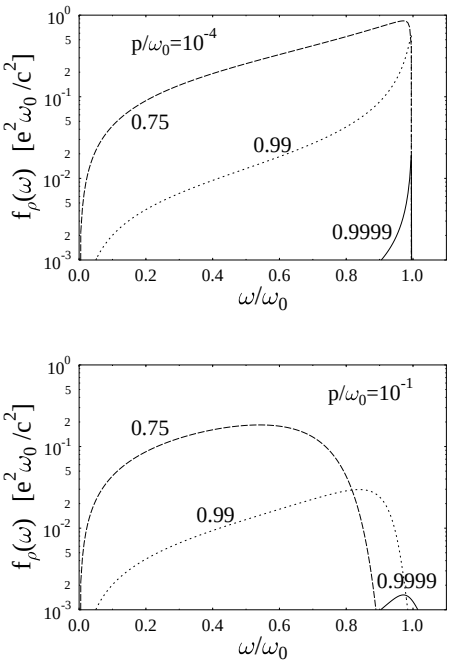

Fig. 6. Spectral distributions of the radiated energy losses per unit length of the cylinder C_ρ. The numbers on a particular line means β (β_c=0.999).